

# Transactions Briefs

## A Discrete-Time Approach to the Steady-State and Stability Analysis of Distributed Nonlinear Autonomous Circuits

Jordi Bonet-Dalmau and Pere Palà-Schönwälder

**Abstract**—We present a direct method for the steady-state and stability analysis of autonomous circuits with transmission lines and generic nonlinear elements. With the discretization of the equations that describe the circuit in the time domain, we obtain a nonlinear algebraic formulation where the unknowns to determine are the samples of the variables directly in the steady state, along with the oscillation period, the main unknown in autonomous circuits. An efficient scheme to build the Jacobian matrix with exact partial derivatives with respect to the oscillation period and with respect to the samples of the unknowns is described. Without any modification in the analysis method, the stability of the solution can be computed *a posteriori* constructing an implicit map, where the last sample is viewed as a function of the previous samples. The application of this technique to the time-delayed Chua's circuit (TDCC) allows us to investigate the stability of the periodic solutions and to locate the period-doubling bifurcations.

**Index Terms**—Autonomous circuits, bifurcation points, distributed, nonlinear, steady-state response, stability analysis, time-domain discretization.

### I. INTRODUCTION

Several techniques have been developed to determine the steady-state response of nonlinear circuits [1]–[4]. In this paper, we first extend the discrete-time approach proposed in [5] to nonlinear autonomous circuits with transmission lines.

Once a solution has been obtained, the next step is to investigate its stability. The solutions computed using integration methods are inherently stable. This is not true when the steady-state response is computed using a direct method. Using the harmonic balance approach, stability may be investigated using perturbation techniques [6] or from a continuation point of view [7]. In this paper, an efficient method to compute the stability of the solutions obtained using the discrete-time approach is presented.

### II. EQUATIONS FORMULATION

Consider an autonomous circuit with only one bias source, one nonlinear element, and one transmission line to achieve a greater insight in the formulation of the equations.

Since the two port resulting from the extraction of the bias source  $v_b$  and the nonlinear element  $f(x)$  is linear, we may apply superposition in the transformed domain, expressing the control variable  $x$  of the nonlinearity in the form

$$X(s) = H_1(s, e^{-s\tau})F(X) + H_2(s, e^{-s\tau})V_b(s) \quad (1)$$

where  $H_j(s, e^{-s\tau}) = -B_j(s, e^{-s\tau})/A(s, e^{-s\tau})$ . With this notation, we rewrite (1) as

$$A(s, e^{-s\tau})X(s) + B_1(s, e^{-s\tau})F(X)$$

$$+ B_2(s, e^{-s\tau})V_b(s) = 0. \quad (2)$$

It is worth emphasizing that  $B_j(s, e^{-s\tau})$  and  $A(s, e^{-s\tau})$  are bivariate polynomials of the following kind:

$$P(s, e^{-s\tau}) = \sum_{i=0}^n \sum_{k=0}^2 p_{ik} s^i e^{-sk\tau}$$

being  $n$  the order of the lumped linear multipoint and  $\tau$  the delay of the transmission line.

### III. EQUATIONS DISCRETIZATION

The operator defined by the polynomial  $P(s, e^{-s\tau})$  applied to the Laplace transform  $U(s)$  of a generic variable  $u(t)$  can be expressed in the time domain as

$$P(s, e^{-s\tau})U(s) \xrightarrow{\text{ILT}} \sum_{i=0}^n \sum_{k=0}^2 p_{ik} \frac{d^i(u(t-k\tau))}{dt^i}. \quad (3)$$

First we will separately discretize each one of the operators, derivation and delay, that appear in (3).

#### A. Computation of the Derivative

In the  $g$ -order Gear method the derivative is approximated at the instant  $n\Delta$  interpolating  $u(t)$  by a polynomial of degree  $g$  fitted to the latest  $g+1$  samples [8]. Thus, defining the vector of the  $N$  samples of a  $T$ -periodic variable  $u(t)$

$$\mathbf{u} = [u_1, u_2, \dots, u_N]^T, \quad \text{with } u_n = u(n\Delta), \quad \Delta = T/N$$

we can approximate the vector of the samples of  $d(u(t))/dt$

$$\dot{\mathbf{u}} = [\dot{u}_1, \dot{u}_2, \dots, \dot{u}_N]^T \quad \text{from} \quad \left. \frac{d(u(t))}{dt} \right|_{t=n\Delta} \approx \dot{u}_n = \sum_{r=0}^g c'_r u_{n-r} \quad (4)$$

where the coefficients  $c'_r$  are obtained from the polynomial fitting procedure described above. For the subsequent calculation of the Jacobian matrix, the dependence of the coefficients  $c'_r$  on the period  $T$  must be stated explicitly. This dependence turns out to be

$$c'_r = \frac{1}{\Delta} c_r = \frac{N}{T} c_r$$

where the coefficients  $c_r$  depend only on the order of the Gear discretization used.

Applying the discretization (4), the derivative operation that appears in (3) can be written as the product of a matrix  $\mathbf{P}_{10}(T)$  by a vector  $\mathbf{u}$ . Thus, we can compute the derivative of  $u(t)$  ( $i = 1, k = 0$  in (3)) as

$$\frac{d(u(t))}{dt} \xrightarrow{g,N} \dot{\mathbf{u}} = \mathbf{P}_{10}(T)\mathbf{u}$$

where

$$\mathbf{P}_{10}(T) = \text{circ}(c'_0, c'_1, \dots, c'_g, 0_{g+1}, \dots, 0_{N-1})^T = \frac{\mathbf{C}}{\Delta} \quad (5)$$

with  $\mathbf{C}$ , independent of  $T$ , as

$$\mathbf{C} = \text{circ}(c_0, c_1, \dots, c_g, 0_{g+1}, \dots, 0_{N-1})^T$$

Manuscript received January 21, 1999; revised June 10, 1999. This paper was recommended by Associate Editor V. V. Perez.

The authors are with the Department of Signal Theory and Communications, Escola Universitària Politècnica de Manresa, Universitat Politècnica de Catalunya, 08240 Manresa, Barcelona, Spain (e-mail: bonet@tsc.upc.es.)

Publisher Item Identifier S 1057-7122(00)01827-4.

where the notation

$$\text{circ}(a_0, a_1, \dots, a_{N-1})^T = \begin{bmatrix} a_0 & a_{N-1} & \cdots & a_1 \\ a_1 & a_0 & \cdots & a_2 \\ \vdots & \vdots & \ddots & \vdots \\ a_{N-1} & a_{N-2} & \cdots & a_0 \end{bmatrix}.$$

The nonzero elements of  $\mathbf{C}$

$$\mathbf{c}_g = [c_0, c_1, \dots, c_g] \quad (6)$$

are given in Table I.

### B. Computation of the $k\tau$ Seconds Delayed Function

Since the  $k\tau$  seconds delayed function evaluated at the instant  $n\Delta$ , i.e.,  $u(n\Delta - k\tau)$ , does not generally coincide with one of the samples, its value is obtained by interpolating  $u(t)$  by a polynomial of degree  $g$  fitted to the sample that follows the instant  $n\Delta - k\tau$  and the  $g$  previous samples. So, we can compute the vector of the samples of  $u(t - k\tau)$

$$\begin{aligned} \mathbf{u}_k &= [u_{k1}, u_{k2}, \dots, u_{kN}]^T \quad \text{from} \\ u(n\Delta - k\tau) &\approx u_{kn} = \sum_{r=0}^g d'_{kr} u_{n-qk-r} \end{aligned} \quad (7)$$

where  $q_k$  is defined according to  $\Delta$  and  $\tau$  as

$$q_k \Delta \leq k\tau < (q_k + 1)\Delta$$

and the coefficients  $d'_{kr}$  are obtained from the polynomial fitting procedure described above. The dependence of the coefficients  $d'_{kr}$  on the period  $T$  turns out to be

$$d'_{kr} = \sum_{j=0}^g d_{rj} (e_k)^j \quad (8)$$

with

$$e_k = \frac{k\tau - q_k \Delta}{\Delta} = N \frac{k\tau}{T} - q_k$$

where the coefficients  $d_{rj}$  depend only on the order of the Gear discretization used.

Applying the discretization (7), the delay operation that appears in (3) can be written as the product of a matrix  $\mathbf{P}_{0k}(T)$  by a vector  $\mathbf{u}$ . So, we can compute  $u(t)$  delayed  $k\tau$  s as ( $i = 0, k$  in (3))

$$u(t - k\tau) \xrightarrow{g, N} \mathbf{u}_k = \mathbf{P}_{0k}(T) \mathbf{u}$$

where

$$\begin{aligned} \mathbf{P}_{0k}(T) &= \text{circ}(0_0, \dots, 0_{q_k-1}, d'_{k0}, \dots, d'_{kg}, 0_{q_k+g+1}, \dots, 0_{N-1})^T \quad (9) \end{aligned}$$

and where the dependence of each coefficient  $d'_{kr}$  on the above defined  $e_k$  can be written, according to (8), as

$$\begin{bmatrix} d'_{k0} \\ d'_{k1} \\ \vdots \\ d'_{kg} \end{bmatrix} = \begin{bmatrix} d_{00} & d_{01} & \cdots & d_{0g} \\ d_{10} & d_{11} & \cdots & d_{1g} \\ \vdots & \vdots & \ddots & \vdots \\ d_{g0} & d_{g1} & \cdots & d_{gg} \end{bmatrix} \cdot \begin{bmatrix} (e_k)^0 \\ (e_k)^1 \\ \vdots \\ (e_k)^g \end{bmatrix}$$

or in compact form

$$\mathbf{d}_k(T) = \mathbf{D}_g \mathbf{e}_k(T). \quad (10)$$

The matrix  $\mathbf{D}_g$ , which is independent of both  $T$  and  $k$ , is given in Table II.

TABLE I  
VECTORS RELATED TO THE DERIVATIVE  
OPERATOR

Discretization order	Vectors in (6)
1	$\mathbf{c}_1 = [1 \quad -1]$
2	$\mathbf{c}_2 = \frac{1}{2} \cdot [3 \quad -4 \quad 1]$
3	$\mathbf{c}_3 = \frac{1}{6} \cdot [11 \quad -18 \quad 9 \quad -2]$
4	$\mathbf{c}_4 = \frac{1}{24} \cdot [50 \quad -96 \quad 72 \quad -32 \quad 6]$

### C. Resulting System of Equations

Now, the discretization of (3) results in

$$\sum_{i=0}^n \sum_{k=0}^2 p_{ik} \frac{d^i(u(t - k\tau))}{dt^i} \xrightarrow{g, N} \mathbf{P}(T) \mathbf{u} \quad (11)$$

with

$$\mathbf{P}(T) \mathbf{u} = \sum_{i=0}^n \sum_{k=0}^2 p_{ik} \mathbf{P}_{ik}(T) \mathbf{u} \quad (12)$$

where it is possible to decompose  $\mathbf{P}_{ik}(T)$  in terms of the matrices (5) and (9) as

$$\mathbf{P}_{ik}(T) = \mathbf{P}_{i0}(T) \mathbf{P}_{0k}(T) = (\mathbf{P}_{10}(T))^i \mathbf{P}_{0k}(T). \quad (13)$$

If we apply the idea contained in (11) to each of the products that appear in (2), we obtain an equivalent formulation in the form

$$\mathbf{A}(T) \mathbf{x} + \mathbf{B}_1(T) \mathbf{f}(\mathbf{x}) + \mathbf{B}_2(T) \mathbf{v}_b = 0 \quad (14)$$

where each matrix only depends on  $T$ , once the order of discretization has been chosen, and is similar in form to  $\mathbf{P}(T)$  defined in (12).

Since in autonomous circuits the period  $T$  is unknown, the system (14) has an infinite number of solutions [5]. From now on, one of the samples of the control variable  $x$  is fixed to a value which, *a priori*, the solution is expected to take.

## IV. COMPUTATION OF THE SENSITIVITIES

Solving (14) efficiently requires to use globally convergent algorithms based on Newton's method [9]. Thus, partial derivatives with respect to the  $N$  unknowns of the system ( $T, x_2, x_3, \dots, x_N$ ) have to be computed.

### A. Partial Derivatives with Respect to the Period

To compute the derivative with respect to the period  $T$  we will previously compute the Jacobian matrix of (12). Since the samples of  $u(t)$  do not depend on the period  $T$ ,

$$\dot{\mathbf{P}}(T) \mathbf{u} = \sum_{i=0}^n \sum_{k=0}^2 p_{ik} \dot{\mathbf{P}}_{ik}(T) \mathbf{u}.$$

Using (13) and the chain rule, we express

$$\dot{\mathbf{P}}_{ik}(T) = \dot{\mathbf{P}}_{i0}(T) \mathbf{P}_{0k}(T) + P_{i0}(T) \dot{\mathbf{P}}_{0k}(T). \quad (15)$$

The computation of the derivative that appears in the first product is computed using (5) as

$$\dot{\mathbf{P}}_{i0}(T) = \frac{-i}{T} \mathbf{P}_{i0}(T).$$

For the computation of the derivative that appears in the second product of (15), we must recall the dependence of  $\mathbf{P}_{ok}(T)$  on  $\mathbf{e}_k(T)$  according to (9) and (10). First, we may write

$$\begin{aligned} \dot{\mathbf{P}}_{ok}(T) &= \text{circ}(0_0, \dots, 0_{q_k-1}, \dot{d}'_{k0}, \dots, \dot{d}'_{kg}, 0_{q_k+g+1}, \dots, 0_{N-1})^T. \end{aligned}$$

Now, using (10), the vector

$$\dot{\mathbf{d}}'_k(T) = [\dot{d}'_{k0}, \dot{d}'_{k1}, \dots, \dot{d}'_{kg}]^T$$

may be expressed as

$$\dot{\mathbf{d}}'_k(T) = \mathbf{D}_g \dot{\mathbf{e}}_k(T) = \frac{-1}{T} \mathbf{D}_g \mathbf{Q}_k \mathbf{e}_k(T)$$

with

$$\mathbf{Q}_k = \begin{bmatrix} 0 & 0 & 0 & \cdots & 0 \\ q_k & 1 & 0 & \ddots & \vdots \\ 0 & 2q_k & 2 & \ddots & 0 \\ \vdots & \ddots & \ddots & \ddots & 0 \\ 0 & \cdots & 0 & gq_k & g \end{bmatrix}$$

defined in terms of the  $g$  order of the Gear discretization used and  $q_k$ .

Once the matrices  $\dot{\mathbf{P}}_{ik}(T)$  have been computed, the computation of  $\dot{\mathbf{B}}_1(T)$ ,  $\dot{\mathbf{B}}_2(T)$  and  $\dot{\mathbf{A}}(T)$  of (14) is straightforward since  $\mathbf{B}_1(T)$ ,  $\mathbf{B}_2(T)$  and  $\mathbf{A}(T)$  are a linear combination of the matrices  $\mathbf{P}_{ik}(T)$ . Thus, the first column of the Jacobian matrix is expressed analytically as

$$\mathbf{J}(:, 1) = \dot{\mathbf{A}}(T)\mathbf{x} + \dot{\mathbf{B}}_1(T)\mathbf{f}(\mathbf{x}) + \dot{\mathbf{B}}_2(T)\mathbf{v}_b.$$

### B. Partial Derivatives With Respect to the Samples

The rest of the columns of the Jacobian matrix are easily determined since only the vectors  $\mathbf{x}$  and  $\mathbf{f}(\mathbf{x})$  depend on the  $N - 1$  unknown samples and their partial derivatives are immediate. So, the remaining columns of the Jacobian matrix are expressed analytically as

$$\mathbf{J}(:, 2 : N) = \mathbf{A}(:, 2 : N) + \mathbf{B}_1(:, 2 : N)\mathbf{F}'(\mathbf{x})$$

with

$$\mathbf{F}'(\mathbf{x}) = \text{diag}(f'(x_2), \dots, f'(x_N))$$

where

$$f'(x_k) = \left. \frac{d(f(x))}{dx} \right|_{x=x_k}.$$

## V. STABILITY ANALYSIS

The stability of the solution obtained can be determined *a posteriori* with no modification to the method described to analyze the circuit. Using the matrices that appear in (14), we can express any of the  $N$  equations as

$$\sum_{k=0}^m a_k x_{n-k} + \sum_{k=0}^m b_k f(x_{n-k}) + c = 0 \quad (16)$$

TABLE II  
MATRICES RELATED TO THE DELAY OPERATOR

Discretization order	Matrices in (10)
1	$\mathbf{D}_1 = \begin{bmatrix} 1 & -1 \\ 0 & 1 \end{bmatrix}$
2	$\mathbf{D}_2 = \frac{1}{2} \begin{bmatrix} 2 & -3 & 1 \\ 0 & 4 & -2 \\ 0 & -1 & 1 \end{bmatrix}$
3	$\mathbf{D}_3 = \frac{1}{6} \begin{bmatrix} 6 & -11 & 6 & -1 \\ 0 & 18 & -15 & 3 \\ 0 & -9 & 12 & -3 \\ 0 & 2 & -3 & 1 \end{bmatrix}$
4	$\mathbf{D}_4 = \frac{1}{24} \begin{bmatrix} 24 & -50 & 35 & -10 & 1 \\ 0 & 96 & -104 & 36 & -4 \\ 0 & -72 & 114 & -48 & 6 \\ 0 & 32 & -56 & 28 & -4 \\ 0 & -6 & 11 & -6 & 1 \end{bmatrix}$

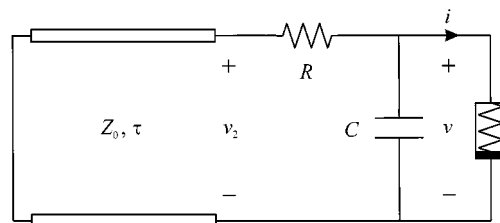


Fig. 1. The time-delayed Chua's circuit (TDCC).

where  $a_k$  and  $b_k$  are the elements of the  $k$ th row of the first column of the matrixes  $\mathbf{A}(T)$  and  $\mathbf{B}_1(T)$ , respectively. Defining

$$\mathbf{x}_n = [x_n, x_{n-1}, \dots, x_{n-m+1}]^T.$$

Equation(16) may be viewed as an implicit map

$$\mathbf{x}_{n+1} = \varphi(\mathbf{x}_n).$$

In this map, the sample  $x_n$  is expressed as a function of the  $m$  previous samples, being  $m$  the memory of the discretized system of equations

$$m \leq q_2 + ng.$$

Once a periodic solution  $\mathbf{x}^*$  of period  $T = N\Delta$  has been found using the technique described, any  $m$  subvector of  $\mathbf{x}^*$  is a fixed point of the composite map  $\varphi^N$ . Now, the natural way to study the stability of this solution is to perturbate it and observe its evolution after one period. This evolution is inferred from the Jacobian of the composite map

$$\mathbf{J} = \mathbf{J}_{N+1}\mathbf{J}_N \cdots \mathbf{J}_2 \quad (17)$$

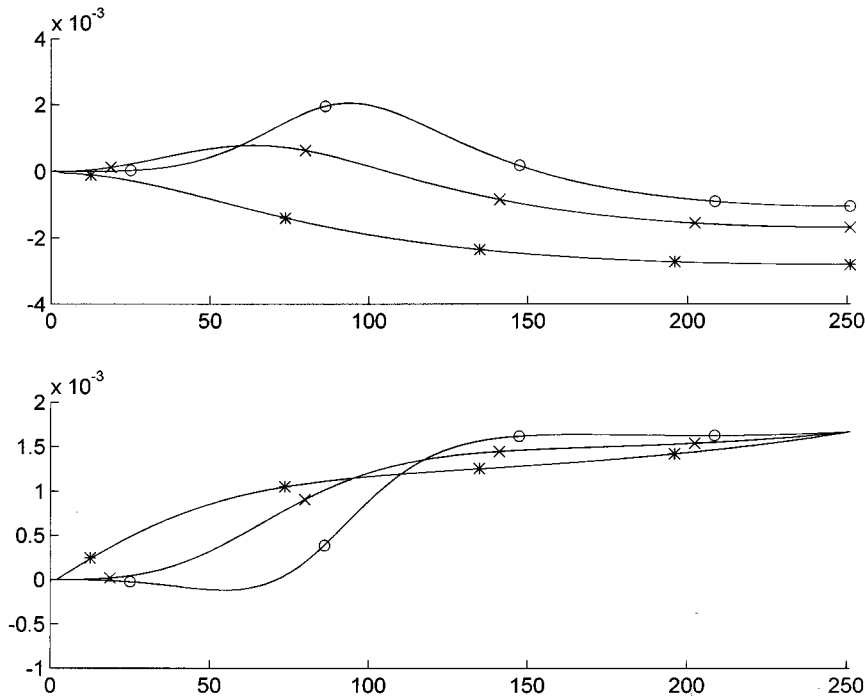


Fig. 2. Relative error in the real part (above) and absolute error in the imaginary part (below) of the eigenvalues in the  $s$  plane for a zero solution with respect to [11] with  $N = 512$  and  $R = 1.85$  k $\Omega$ . Gear-2 (\*), Gear-3 (x), Gear-4 (o).

where

$$\mathbf{J}_n = \begin{bmatrix} \frac{\partial x_n}{\partial x_{n-1}} & \frac{\partial x_n}{\partial x_{n-2}} & \cdots & \frac{\partial x_n}{\partial x_{n-m+1}} & \frac{\partial x_n}{\partial x_{n-m}} \\ 1 & 0 & \cdots & 0 & 0 \\ 0 & 1 & & & 0 \\ \vdots & & \ddots & & \vdots \\ 0 & 0 & & 1 & 0 \end{bmatrix}$$

and

$$\frac{\partial x_n}{\partial x_{n-k}} = -\frac{a_k + b_k f'(x_{n-k})}{a_0 + b_0 f'(x_n)}.$$

Now, the eigenvalues of the Jacobian  $\mathbf{J}$  defined in (17) give direct information about the stability of the solution: 1) for autonomous circuits  $\mathbf{J}$  has unity as eigenvalue since this type of circuits admit infinite shifted solutions; 2) if the remaining eigenvalues are smaller than unity in modulus, then the periodic solution is stable; and 3) the solution is unstable if  $\mathbf{J}$  has at least one eigenvalue with a modulus greater than unity. Other eigenvalues whose modulus is equal to unity correspond to special cases. In particular, an eigenvalue equal to  $-1$  indicates the existence of a period-doubling bifurcation point.

In [10], the relation between the eigenvalues of  $\mathbf{J}$  and the eigenvalues of the monodromy matrix is stated for lumped circuits.

## VI. APPLICATION TO THE TIME-DELAYED CHUA'S CIRCUIT

The technique described has been applied to the determination of the steady state of the control variable  $v$  in the time-delayed Chua's circuit (TDCC) shown in Fig. 1. The values of the parameters which appear in the circuit are the same used in [11]. For numerical accuracy reasons, these parameters have been normalized with  $R_0 = 1$  k $\Omega$  and  $T_0 = 0.1$  ms.

For the determination of the periodic solution, the second-order Gear discretization has been used because it has shown to be a good compromise between accuracy and computational cost.

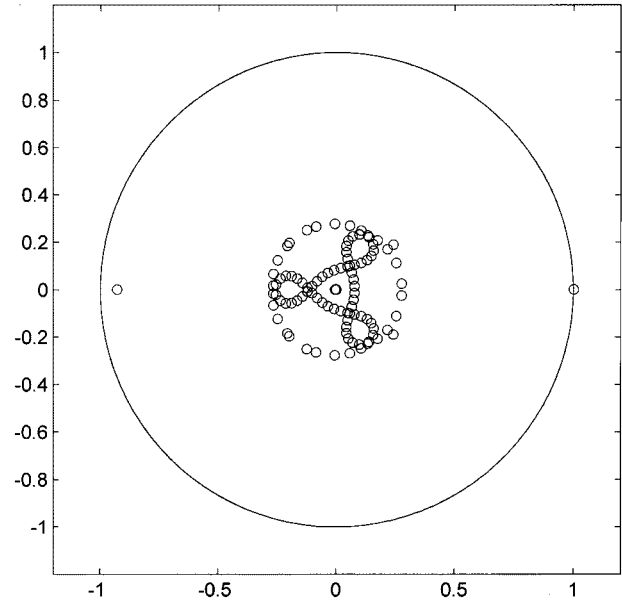


Fig. 3. Eigenvalues in the  $z$ -plane for a stable period-1 limit cycle with  $N = 256$ ,  $R = 1.8038$  k $\Omega$  and  $g = 2$ .

### A. Equilibrium Points

The purpose of this section is to check the accuracy of the procedure that has been described contrasting the results with those obtained analytically at the equilibrium points. If  $R = 1.85$  k $\Omega$  the system has three equilibrium points:  $v = \{0, +3.861, -3.861\}$ . As these equilibrium points are direct solutions of (2), no iterative solving process is needed. So, only the stability analysis is made in this section.

1) *Zero Equilibrium Point:* Applying the stability study described in the previous section, the eigenvalues in the  $z$ -plane are obtained with  $N = 512$  samples of value zero. All the eigenvalues rest inside the unit

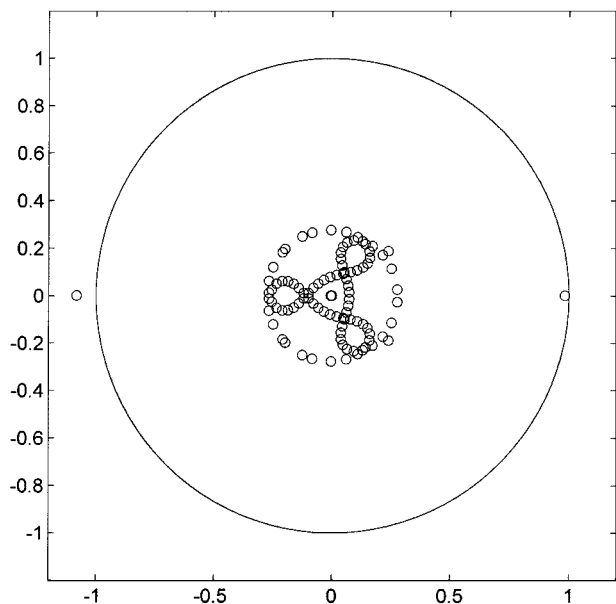


Fig. 4. Eigenvalues in the  $z$ -plane for an unstable period-1 limit cycle with  $N = 256$ ,  $R = 1.8037$  k $\Omega$ , and  $g = 2$ .

circle, except one that is outside, of value  $z = 130$  for a second-order Gear discretization. So, zero is an unstable solution.

Applying the transformation  $z = e^{sT}$  our stability study can be translated to the  $s$  plane as in [11]. Figure 2 shows excellent agreement between the analytical and the numerical method for a second to fourth-order Gear discretization.

2) *Nonzero Equilibrium Points*: Repeating the same stability analysis for the nonzero equilibrium points we observe that all the eigenvalues in the  $z$  plane rest inside the unit circle. Therefore the solution is stable. These equilibrium points become unstable when  $R$  is reduced to 1.82 k $\Omega$ . So, for  $R \leq 1.82$  k $\Omega$  a periodic solution is expected.

**B. Period-1 Limit Cycle**

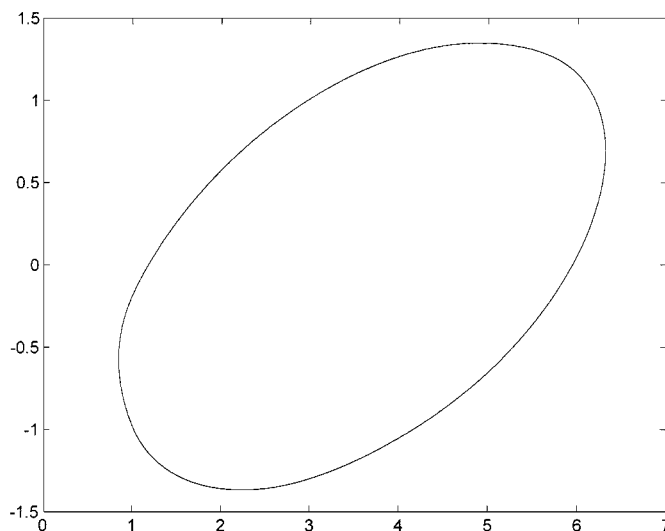
Now we investigate the solution for  $R = 1.82$  k $\Omega$ . Initializing the iterative solving process with  $N = 128$  samples of a sinusoidal signal of amplitude 3 V, period  $5\tau$  and offset 3.861 V, a stable period-1 limit cycle is obtained. This solution is interpolated to obtain  $N = 256$  samples and used as a new initialization. The resulting period-1 phase plane is depicted in Fig. 5. All the eigenvalues related to this solution rest inside the unit circle except one of value equal to one, which indicates that a shifted solution is possible. So, the solution is stable.

Once a solution has been computed, we change the parameter  $R$  to obtain new solutions using as an initialization the previous one. Applying this technique, we reduce  $R$  using 10  $\Omega$  steps until we observe that at  $R = 1.8$  k $\Omega$  the solution obtained is unstable. A more detailed analysis proves that one eigenvalue has crossed the unit circle at  $z = -1$  between  $R = 1.8038$  k $\Omega$  and  $R = 1.8037$  k $\Omega$  as is shown in Figs. 3 and 4. So, a period-doubling bifurcation point is expected.

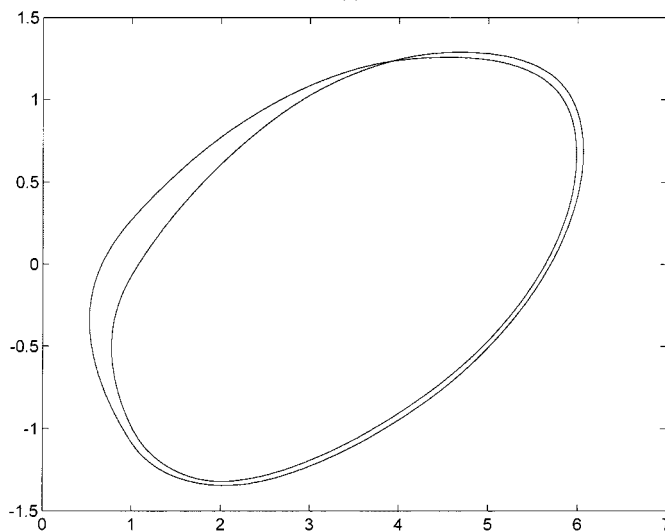
The problem now is to find the stable solution that corresponds to  $R = 1.8037$  k $\Omega$ . From the eigenvector associated to the eigenvalue that has crossed the unit circle, we know the perturbation

$$\mathbf{p}_m = [p_m, p_{m-1}, \dots, p_1]^T$$

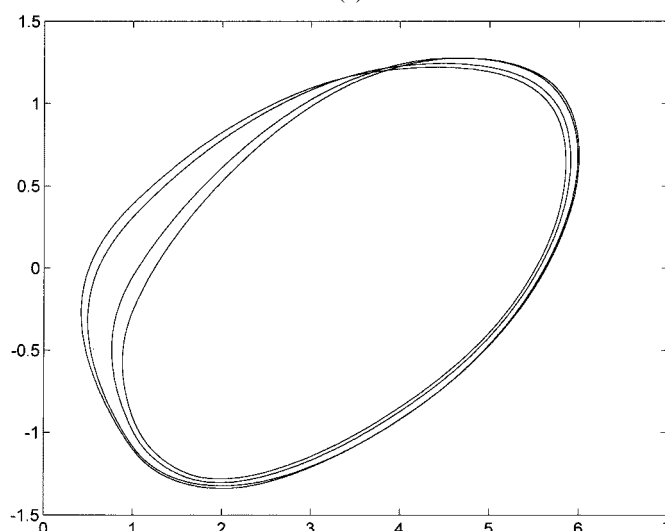
that transforms the period-1 solution into a period-2 solution. However, this eigenvector has only  $m$  samples. The rest of the samples, up to  $2N = 512$ , should be computed to initialize the iterative solving process with two periods of the unstable period-1 solution plus the computed perturbation. If, as expected, the perturbation is small compared



(a)



(b)



(c)

Fig. 5. Phase plane of  $v_2$  versus of  $v$ . (a) a period-1 limit cycle with  $N = 256$ ,  $R = 1.82$  k $\Omega$ , and  $g = 2$ . (b) A period-2 limit cycle with  $N = 512$ ,  $R = 1.8$  k $\Omega$  and  $g = 2$ . (c) A period-4 limit cycle with  $N = 1024$ ,  $R = 1.7952$  k $\Omega$ , and  $g = 2$ .

with the solution, the nonlinear equation (16) can be linearized around the period-1 solution. Consequently, the rest of the samples can be computed using the vector  $\mathbf{p}_m$  and the linear expression

$$p_n = -\frac{\sum_{k=1}^m a_k p_{n-k} + \sum_{k=1}^m b_k f'(x_{n-k}) p_{n-k}}{a_0 + b_0 f'(x_n)} \quad n > m.$$

Once the perturbation vector

$$\mathbf{p} = [p_1, p_2, \dots, p_{2N}]^T$$

of  $2N = 512$  samples has been computed, we obtain a period-2 solution adding the vector  $\mathbf{p}$  multiplied by a constant  $\alpha$  to two periods of the period-1 solution

$$\mathbf{x}_{|\text{period-2}} \approx [\mathbf{x}_{|\text{period-1}}; \mathbf{x}_{|\text{period-1}}] + \alpha \mathbf{p}. \quad (18)$$

If this constant is well chosen, the approximate solution is close to the final solution and the iteration will converge.

### C. Period-2 and Period-4 Limit Cycles

With the initialization proposed in (18) with  $\alpha = 0.6$ , we obtain the phase plane depicted in Fig. 5. The eigenvalues are all inside the unit circle. Therefore the solution is stable. *A posteriori* we can verify the hypothesis made in (18) that the eigenvector  $\mathbf{p}$  added to the period-1 solution is indeed close to the period-2 solution.

With the decrease of the parameter  $R$  over the period-2 solution a new period doubling bifurcation point is detected for  $R = 1.796$  k $\Omega$ . A stable period-4 solution is computed for  $R = 1.7952$  k $\Omega$  (Fig. 5).

## VII. CONCLUSION

A new method to directly determine the steady-state response of nonlinear autonomous circuits with distributed parameters has been presented. To validate the method, it has been applied to the analysis of the TDCC in one of its periodic windows, a paradigmatic example of the kind of circuits to which this paper refers.

A procedure for determining the stability of the steady-state solutions is presented. To check the reliability of this method, it has been applied to the stability at the equilibrium points of the TDCC in which analytical results exist [11] and excellent agreement has been obtained.

The combination of the discrete-time approach with the study of the stability of the solutions obtained allows us to detect period-doubling bifurcation points. A procedure to initialize the iterative solving process to obtain the bifurcated solution is explained and successfully applied. The results coincide with those described in [11], and with those obtained using integration techniques, without having to integrate the response until the transient dies out.

## REFERENCES

- [1] V. Rizzoli and A. Neri, "State of the art and present trends in nonlinear microwave CAD techniques," *IEEE Trans. Microwave Theory Tech.*, vol. 36, pp. 343–365, Feb. 1988.
- [2] T. J. Aprille Jr. and T. N. Trick, "Steady-state analysis of nonlinear circuits with periodic inputs," *Proc. IEEE*, vol. 60, pp. 108–114, Jan. 1972.
- [3] G. W. Rhyne, M. B. Steer, and B. D. Bates, "Frequency-domain nonlinear circuit analysis using generalized power series," *IEEE Trans. Microwave Theory Tech.*, vol. 36, pp. 379–387, Feb. 1988.
- [4] K. S. Kundert and A. Sangiovanni-Vincentelli, "Simulation of nonlinear circuits in the frequency domain," *IEEE Trans. Computer-Aided Design*, vol. 5, pp. 521–535, Oct. 1986.
- [5] P. Palà-Schönwälder and J. M. Miró-Sans, "A discrete-time approach to the steady-state analysis and optimization of nonlinear autonomous circuits," *Int. J. Circuit Theory Appl.*, vol. 23, pp. 297–310, 1995.

- [6] V. Rizzoli and A. Lipparini, "General stability analysis of periodic steady-state regimes in nonlinear microwave circuits," *IEEE Trans. Microwave Theory Tech.*, vol. 33, pp. 30–37, Jan. 1985.
- [7] D. Hente and R. H. Jansen, "Frequency domain continuation method for the analysis and stability investigation of nonlinear microwave circuits," *Proc. Inst. Elect. Eng.*, vol. 133, pp. 351–362, Oct. 1986.
- [8] A. M. Schneider, J. T. Kaneshige, and F. D. Groutage, "Higher order s-to-z mapping functions and their application in digitizing continuous-time filters," *Proc. IEEE*, vol. 79, pp. 1661–1674, Nov. 1991.
- [9] J. E. Dennis and R. B. Schnabel, *Numerical Methods for Unconstrained Optimization and Nonlinear Equations*. Englewood Cliffs, NJ: Prentice-Hall, 1983.
- [10] J. M. Miró-Sans, P. Palà-Schönwälder, and O. Mas-Casals, "Stability analysis of periodic solutions in nonlinear autonomous circuits: A discrete-time approach," *Int. J. Circuit Theory Appl.*, vol. 24, pp. 511–517, 1996.
- [11] E. A. Hosny and M. I. Sobhy, "Analysis of chaotic behavior in lumped-distributed circuits applied to the time-delayed Chua's circuit," *IEEE Trans. Circuits Syst. I*, vol. 41, pp. 915–918, Dec. 1994.

## A Low-Voltage Single Input Class AB Transconductor With Rail-To-Rail Input Range

Ahmed A. El-Adawy and Ahmed M. Soliman

**Abstract**—A new CMOS programmable rail-to-rail transconductor is presented. A linear  $V$ - $I$  characteristic is obtained by using the principle of nonlinearity cancellation of matched MOS transistors operating in the ohmic region. Rail-to-rail operation is achieved by using two complementary blocks. The circuit is suitable for low voltage as it can operate from supply voltages down to  $\pm 1.5$  V. PSpice simulations show that the transconductance gain can be electronically tuned from 13 to 90  $\mu$  A/V with bandwidth of about 40 MHz.

**Index Terms**—Low-voltage circuits, transconductors.

## I. INTRODUCTION

As the advances in the VLSI technology and the demand for portable electronic products lead VLSI circuits operating in low supply voltages (lower than 3 V), current-mode signal processing techniques will become increasingly important and attractive [1]–[5]. Circuits designed to exploit the current-mode techniques improve operating speed and can be implemented in low-cost digital CMOS fabrication process. Traditionally, however, most analog signal processing has been accomplished by using voltage as the signal variable. In order to maintain compatibility with voltage processing circuits, it is often necessary to convert the input and output signals of a current-mode signal processor to voltage, that is, to use transconductors (or  $V$ - $I$  converters). Numerous transconductor design schemes have been proposed and implemented [6]–[12]. However, most of these schemes have the problem that the control voltage that controls the transconductance gain also affects the linear operating range. This leads to a conflict between obtaining large input linear range and high transconductance gain. The proposed transconductor has a programmable gain while

Manuscript received September 2, 1998; revised April 13, 1999. This paper was recommended by Associate Editor A. H. M. Van Roermund.

The authors are with the Electronics and Communications Engineering Department, Cairo University, Giza, Egypt.

Publisher Item Identifier S 1057-7122(00)01803-1.